INTERNATIONAL JOURNAL OF OPTIMIZATION IN CIVIL ENGINEERING
Int. J. Optim. Civil Eng., 2020; 10(3):411-431

OPTIMUM LAYOUT OF NONLINEAR FLUID VISCOUS DAMPER FOR IMPROVEMENT THE RESPONSES OF TALL BUILDINGS

A. Shariati[1], R. Kamgar[2] and R. Rahgozar[3*, †]
[1]*Department of Civil Engineering, Seed of Arian Saze Zagros, Chaharmahal Science & Technology Park, Shahrekord, Iran*
[2]*Assistant Professor of Civil Engineering, Shahrekord University, Shahrekord, Iran*
[3]*Professor of Civil Engineering, Shahid Bahonar University of Kerman, Kerman, Iran*

ABSTRACT

The utilization of passive energy dissipation systems has been created a revolution in the structural engineering industry due to their advantages. Fluid Viscous Damper (FVD) is one of these control systems. It has been used in many different industries, such as the army, aerospace, bridge, and building structures. One of the essential questions about this system is how it can combine with the bracing system to enhance its abilities. In this paper, a comparison between the responses of a twelve-story steel building retrofitted by four layouts of bracings systems (i.e., chevron, diagonal, toggle, and X-brace) is studied. These bracing systems are equipped by FVD to find the optimum layout for these systems. Buildings are modeled nonlinearity and excited by an earthquake (Manjil earthquake). For this purpose, the Fast Nonlinear Analysis (FNA) is performed using the SAP2000 software. The results show that FVD alters some of the structural behaviors such as inter-story drift when combining with a chevron-bracing system. As a result, it can decrease the motion induced by the earthquake significantly. Besides, the results show that the chevron model has the best performance for the high-rise building in comparison with the other studied systems. As a result, for toggle, chevron, and diagonal bracing systems, the formation of link damper could absorb 66%, 72%, and 79% of input energy instead of modal damping energy, respectively.

Keywords: Nonlinear dynamic analysis; Fluid viscous damper; Tall building; Earthquake

Received: 25 January 2020; Accepted: 16 May 2020

[*]Corresponding author: Department of Civil Engineering, Shahid Bahonar University of Kerman, Kerman, Iran
[†]E-mail address: rahgozar@uk.ac.ir (R. Rahgozar)

1. INTRODUCTION

There are a variety of vibration control systems to decrease structural responses [1-16]. These control devices are categorized as active, passive, semi-active, and hybrid vibration control systems. FVD system is known as a passive control system, and it does not need an external system to supply the force required to control the vibration of the structure [17]. This paper deals with the FVD to enhance the ability of the tall building against the earthquake load. During the industrial revolution, there are quite creating a mixed variety of dampers to control and decline the structural vibrations. Dampers can absorb a percentage of input energies, and therefore, it can decrease the structural damage [18]. Today, it is vital to find the optimal values in engineering problems [19-26, 9, 27, 12-14].

On the other hand, the knowledge of dampers needs to have a sharp development to recognize their behaviors completely. In this way, there are a few questions as follows:

How many dampers should be utilized in a building structure?

Which type of damper model has the best performance for the structure?

How can structural designers build a model, analyze it, and pursue structural behavior with dampers [28]?

The answers to these questions illustrate the importance of examining the behavior of control systems subjected to the lateral loads. The answer to the second question mentioned above is the main aim of this paper. For this purpose, the FVD is selected as the vibration control system. Fig. 1 shows the schematic of FVD [28].

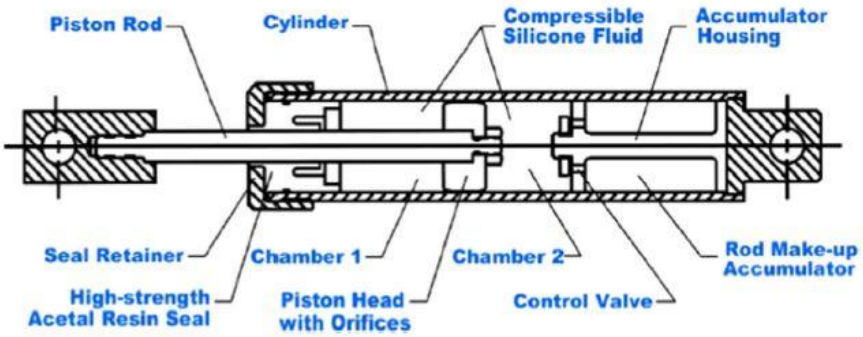

Figure 1. Scheme of fluid viscous damper [28]

It should be noted that the vibration control systems have different engineering applications [29-32]. Lian et al. studied the effect of shear link and bracing systems in the behavior of tall buildings [33-35], especially for the responses of beam and panel zone. Several researchers also investigate the use of the tuned mass damper in minimizing the vibration of structures [36, 37, 11]. They showed that the TMD could reduce the responses of buildings subjected to the earthquake if the optimum parameters are selected for the mass, stiffness, and damping of the TMD.

The evolution of large dampers began in the 1860s [38]. Between World War I and World War II, FVD technology has utilized in military and aerospace applications [28]. However, at the end of the cold war, FVD was used in different industries [38]. Taylor Device Company decided to pursue joint research with the National Center for Earthquake Engineering

Research (NCEER) on utilizing fluid damped in the building and bridge structures. All tests proved an excellent reduction in the values of stress and deflection for the buildings retrofitted by FVD in the range of 15-40%. In general, it was discovered that adding 20% damping to a structure would triple its earthquake resistance, without any increased stress or deflection [38]. The use of FVD for seismic energy dissipation on full-size civil engineering structures commenced in 1993. To date, more than 300 civil engineering structures are now utilizing this technology. Benefits obtained in these constructions are categorized as reducing in cost of the project, decreasing the value of column stresses and deflections, reducing in the using the materials for construction, and preservation of architectural attributes and enhancements. The application of this system is for the first time related to the San Bernardino County Medical Center Replacement Project [39].

It should be noted that a few elements of tall-building will experience the plastic zone while others can stay in the elastic zone subjected to the severe earthquake. So, it is good to use the FVD system for decreasing the value of damage by absorbing the input energy induced by an earthquake. Therefore, after obtaining the best layout for this system to have minimum structural responses, this optimum layout can be used by structural designers and companies.

As time goes on, the researches have shown that FVD has several advantages to resist lateral forces such as earthquake and wind. Due to the lack of sufficient research on using FVD for control vibration of tall buildings, this paper focuses on the effect of this system on reducing the structural responses of tall buildings. For the first time, a twelve-story steel building retrofitted with the X-bracing system is considered and designed. The building is assumed to be symmetric in its plan. Then, three-different other layouts for FVD are considered, remodeled, and designed instead of the X-bracing system against the earthquake. Finally, a comparison between the structural dynamic responses of different models is performed. It can be concluded that which layout of FVD has the best performance.

2. FLUID VISCOUS DAMPER

FVD devices consist of a cylinder containing a high viscosity fluid, as sketched in Fig. 1 [40]. It produced a force that always resists against the motion of the structure. This force is related to the relative velocity between the structure and damper. In this type of damper, the damping law can be written as follows:

$$F = CV^{\alpha} \tag{1}$$

where F, C, V and α are the damping force, a damping coefficient, the relative velocity, and the velocity exponent in the range of $0.3 < \alpha < 1.95$ (α remains constant over the full range of velocities) [28].

For $\alpha = 1$, it is called linear FVD; on the other hand, when $\alpha < 1$, this leads to create a nonlinear FVD, which is useful in minimizing high-velocity shocks. The most important results of published researches show that the effect of the nonlinearity is higher for lower values of α. The values of α in the range of 0.2-0.3 are more effective since the envelopes of

acceleration, and inter-story drifts are most not modified using the α value close to one [41]. Fig. 2 shows the relation between the F and V parameters for different values of α.

Furthermore, the research proves that the most popular value of α is in the range of 0.3 to 0.5 for the seismic building designs. Besides, this value varies in the range of 0.5-1.0 for the massive structures subjected to the wind load. Therefore the lower values of α should be used since a structure must withstand both wind and earthquake loads [38]. Also, Fig. 3 shows the relation between the damping force and displacement for different types of FVD [18]. Fig. 3 proves that the behavior of FVD approaches to the Friction Damper (FD) when the value of α increases.

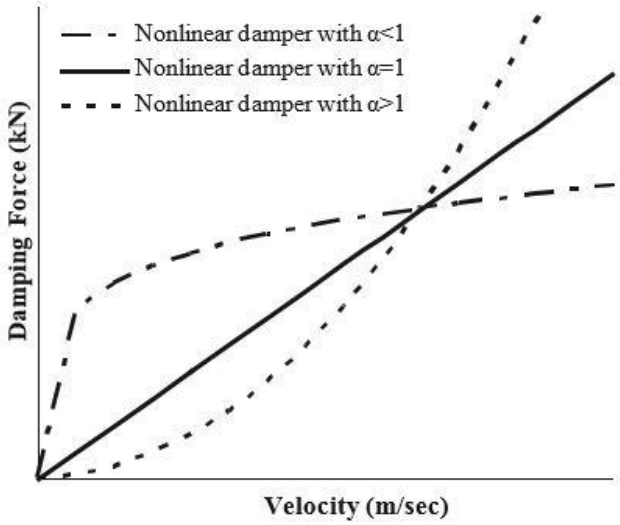

Figure 2. The relation between damping force and relative velocity for different values of α [18]

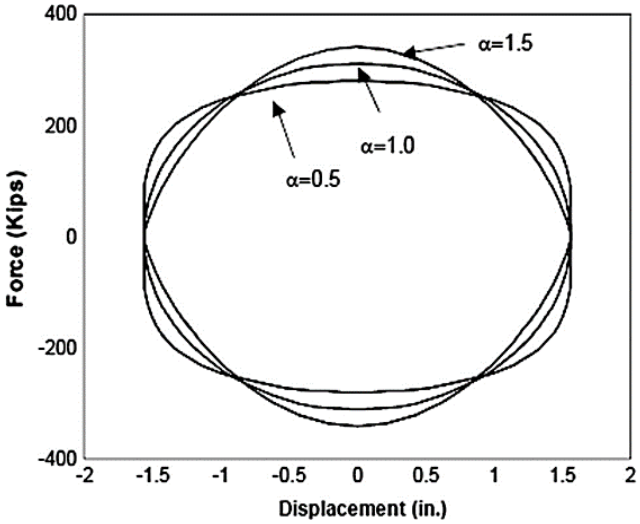

Figure 3. The relation between force and displacement for different FVD systems [18]

3. ABILITIES OF SAP2000 SOFTWARE

The structural engineers are trying to analyze the structures by the use of real forces such as earthquakes and wind. However, there is a lot of software to analyze building structures. SAP2000 is one of the most powerful software, not only having a comprehensive library for different dampers but also can create static and dynamic analysis methods for structural analysis. Additionally, it can model structures with high flexibility [17]. FVD exhibits viscoelastic behavior, which can be predicted with the Kelvin and Maxwell models for linear and nonlinear analysis, respectively [18] (see Fig. 4).

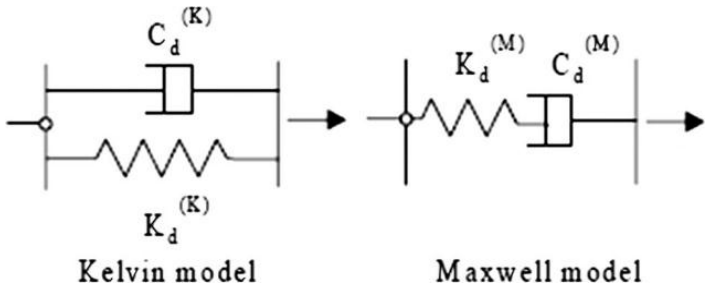

Figure 4. Kelvin and Maxwell models [18]

It should be mentioned that there are two nonlinear dynamic methods involving nonlinear modal analysis and nonlinear direct integration analysis methods [42]. In this paper, the direct-integration time history analysis method is used to perform a nonlinear time history analysis for FVD [43]. Overall, the SAP2000 software is used to model the structure since it can make a three-dimensional model of the structure with the FVD system. Also, this software can perform the FNA as an appropriate option for modeling of building structures.

4. CASE STUDY

4.1. Structural loads

It is assumed that the building is located in the Olympia (site class D) and, therefore, using ASCE07-10 standard [44], the required information is extracted for getting the needed accelerograms at PEER Ground Motion Database [45]. Tables (1-2) show the obtained data and introduce eight accelerograms obtained based on parameters shown in Table 1.

Table 1: Parameters for the site of the building based on ASCE07-10 [44]

S_S	**1.25**	**S_{DS}**	**0.83**	**S_{MS}**	**1.25**
S_1	**0.60**	**S_{D1}**	**0.69**	**S_{M1}**	**0.90**

where S_S, S_1, S_{DS}, S_{D1}, S_{MS}, and S_{M1} are the mapped MCER (Maximum Considered Earthquake), 5% damped, spectral response acceleration parameter at short periods, the mapped MCER, 5% damped, spectral response acceleration parameter at a period of 1 (sec),

the design, 5% damped, spectral response acceleration parameter at short periods, the design, 5% damped, spectral response acceleration parameter at a period of 1 (sec), the MCER, 5% damped, spectral response acceleration parameter at short periods adjusted for site class effects, and the MCER, 5% damped, spectral response acceleration parameter at a period of 1 (sec) adjusted for site class effects, respectively.

Table 2: Summary properties of selected records

ID	Mag.	Earth. Name	Year	Scale Factor	Mech.
1	6.36	Coalinga-01	1983	1.2133	Reverse
2	6.93	Loma Prieta	1989	2.1254	Reverse Oblique
3	7.62	Chi-Chi (Taiwan)	1999	1.7196	Reverse Oblique
4	7.37	Manjil (Iran)	1990	1.2966	Strike-slip
5	7.13	Hector Mine	1999	0.7472	Strike-slip
6	6.8	Chuetsu Oki (Japan)	2007	1.7952	Reverse
7	6.9	Iwate (Japan)	2008	1.0934	Reverse
8	7.0	Darfield (New Zealand)	2010	2.5102	Strike-slip

where Mag. and Mech. Depict the magnitude and fault movement mechanism, respectively.

4.2. Structural modeling

Firstly, a twelve-story steel tall building retrofitted by the X-brace system (see Figs. 5-6) is analyzed and designed subject to the eight earthquakes shown in Table 2. The *ST37* material is considered for the structural elements. However, the results depict that the Manjil earthquake is the best candidate for this structure. The requires lateral stiffness and damping for different lateral resistance system, and each story is shown in Tables (3-4). It should be mentioned based on Ras and Boumechra research [18], it is better to decrease the parameter C when the height of structure increases. Therefore, the damping value of FVD has been decreased by increasing the height of the structure (see Tables 3-4)

Besides, in this paper, four scenario states are considered for the structure (see Fig. 7). It should be noted that there is no any FVD installed on the x bracing system. The FVD system is only installed for diagonal, chevron, and toggle bracing systems. Some specifications are completely similar for all considered scenarios as follows:

1- The bracing systems are installed only in the y-direction. Therefore, the systems are considered to be a dual system in the y-direction.

2- The moment-resisting frame system is placed in the x-direction.

3- The center of mass is close to the center of stiffness.

The four considered scenarios are modeled and analyzed subjected to the Manjil earthquake. Additionally, to eliminate the torsion in the FVD elements, it is essential to consider a stiffness for the FVD system that the stiffness value should be more than that of the X-bracing system. Therefore, the stiffness values of the FVD systems are also decreased by increasing the height of the structure (see Table 3). Besides, Figs. (8-9) indicate the relationships between the damping force and velocity for the linear and nonlinear FVD systems, respectively. It should be mentioned that in this paper, the value of α is considered to be equal to 0.5 for all FVD systems [46]. Therefore, according to Table 4, an interval is

calculated for all three floors for the *C* parameter. Finally, the average value of this parameter is selected as the appropriate value that has the highest amount of energy absorption.

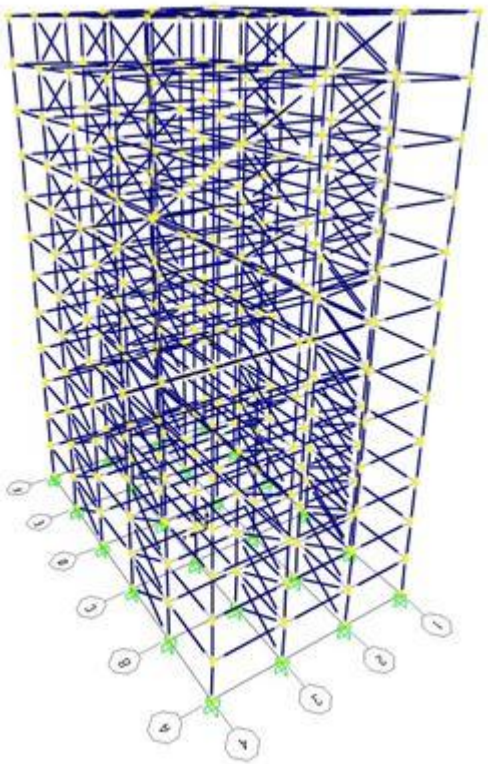

Figure 5. Twelve-story steel building analyzed in SAP2000

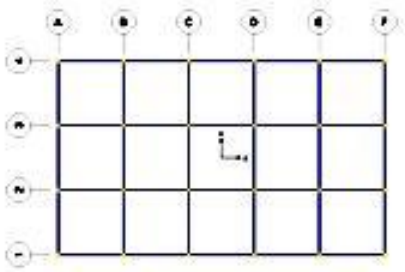

Figure 6. Plan of the studied building

Table 3: Values of calculated stiffness for different lateral resistance systems in the unit (kN/m)

Floor number	X-brace	Diagonal damper	Chevron damper	Toggle damper
10^{th} - 12^{th}	261865	261865	265000	265000
7^{th} - 9^{th}	290063	290063	300000	300000
4^{th} - 6^{th}	331040	331040	340000	340000
1^{th} - 3^{th}	366222	366222	370000	370000

Table 4: The axial force (kN) and the damping coefficient (kN.s/m)

Floor number	The axial force of X-brace	Damping coefficient
10^{th} - 12^{th}	260	184<C<581
7^{th} - 9^{th}	400	283<C<894
4^{th} - 6^{th}	520	368<C<1163
1^{th} - 3^{th}	550	338<C<1230

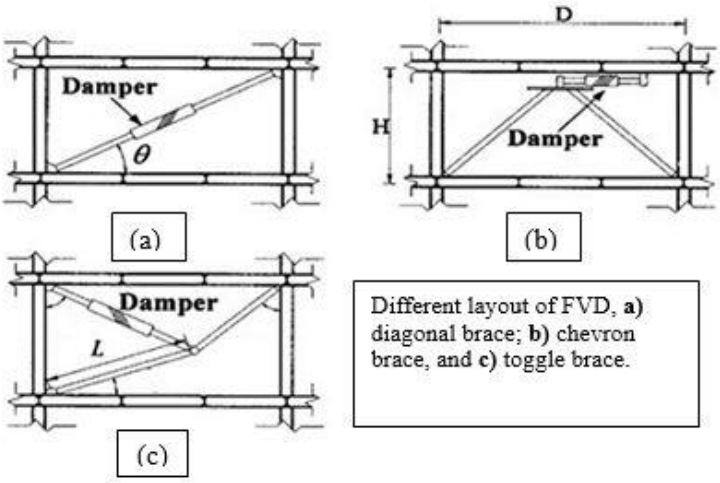

Figure 7. All studied layout of FVD

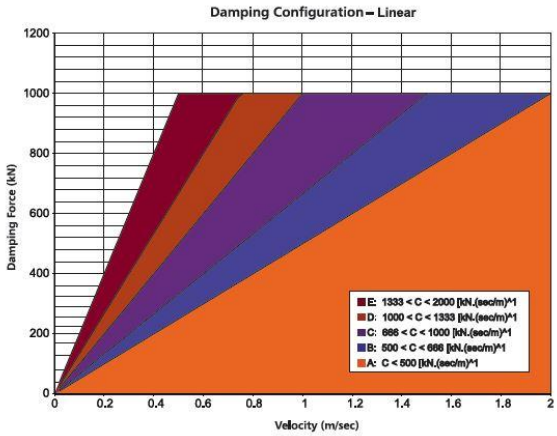

Figure 8. Relationships between the damping force and relative velocity for the linear FVD systems [46]

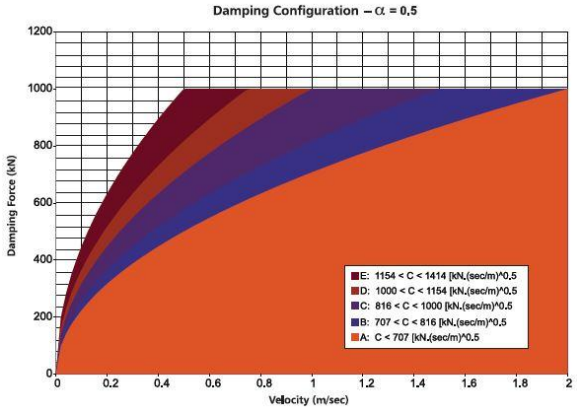

Figure 9. Relationships between the damping force and relative velocity for the nonlinear FVD systems [46]

Based on Figs. (8-9) and also, the obtained results from SAP2000, the damping coefficients are calculated and listed in Table 4. As shown in this table, the damping coefficient of the FVD system should be decreased when the height of the building is increased. This action leads to having a more economical project, and also the FVD system used efficiently [18]. It is be noted that in Table 4, the value of velocity is in the range of 0.2 to 2 (m/sec).

5. RESULTS AND THEIR INTERPRETATION

In this section, the responses of the studied models are compared with each other to obtain the best layout of the FVD system for a tall building. The acceleration time history of the floor story is plotted in Fig. 10 for different studied models. It shows that the toggle bracing system that has been equipped with the FVD system has the minimum values of roof acceleration. Also, the X-bracing system has maximum roof acceleration value.

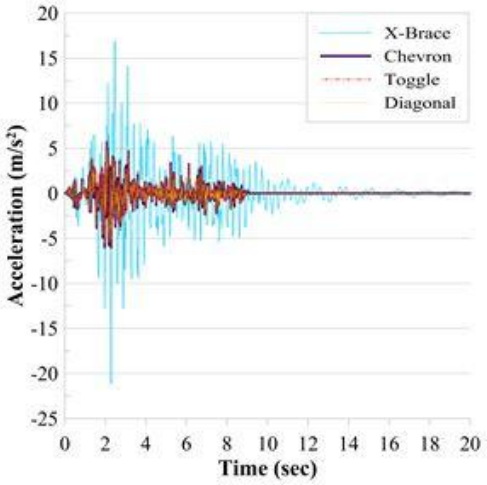

Figure 10. Accelerations time history of the floor story for different studied models

The result indicates that a combination of FVD with the toggle bracing system can reduce the value of roof acceleration by 70% in comparison with the X-bracing system. Besides, it can be concluded that the use of FVD causes to stop the vibration of the controlled structures within 10 to 20 (sec), while in a structure equipped with X-braces (where the FVD system is not used) the structure continues to vibrate during this period.

The displacement time history of the floor story is also depicted in Fig. 11 for different studied models. It shows that the chevron bracing system that has been equipped with the FVD system has the minimum values of roof displacement. Also, the toggle bracing system has maximum roof displacement value. The result indicates that a combination of FVD with the toggle bracing system will increase the value of roof displacement by 22 times that value occurs in the chevron bracing system. Besides, it can be concluded that the use of FVD with the toggle bracing system causes to increase the inelastic deformation in comparison with the other studied systems. In the X-bracing systems, the system fluctuated almost around the elastic state of the system. For the combination of FVD with the diagonal and chevron

bracing systems, the buildings fluctuated around a new inelastic state of the system. Still, the values of inelastic deformation are low.

Investigation of the formation of plastic hinges indicates that some plastic hinges are formed in the toggle bracing system. Therefore, the building can not come back to the first initial configuration after the earthquake, and some structural elements will experience plasticity behavior. Furthermore, a longer wavelength on the displacement response of diagonal and chevron systems is shown that the FVD system can make a slower reaction in comparison with the X-bracing system subjected to the earthquake. As a result, the nonstructural parts will have minimum damage for the chevron and diagonal bracing system.

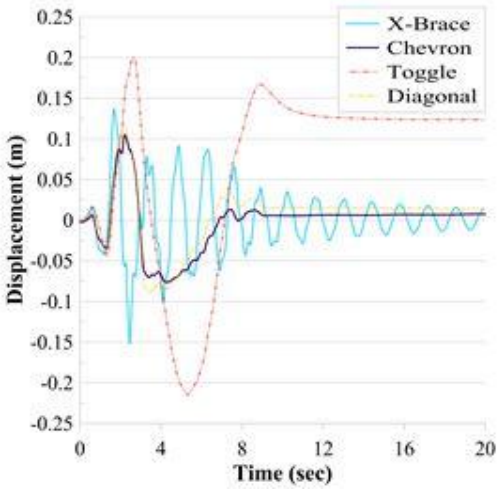

Figure 11. Displacement time history of the floor story for different studied models

Fig. 12 illustrates the values of floor displacements for different values of C. It is evident that the chevron and diagonal bracing systems have almost similar behaviors. The chevron bracing system has the least displacement in comparison with the diagonal bracing systems. The toggle bracing system also has the maximum floor displacements.

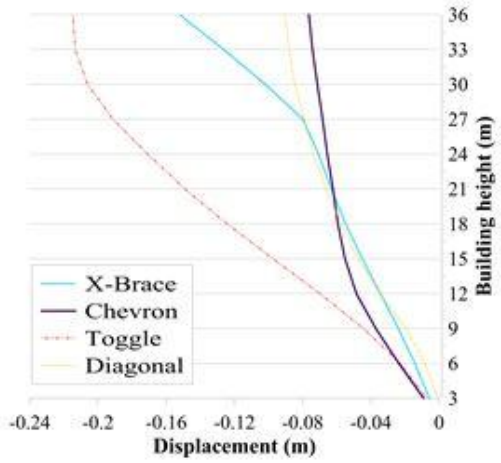

a) Minimum

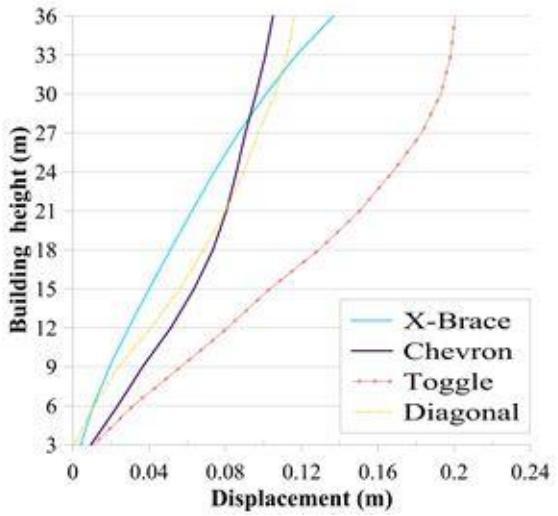

b) Maximum

Figure 12. Variation of floor displacement for minimum and maximum range of C listed in Table 4

Fig. 13 shows the base moment of four studied models. It can be seen that the chevron and diagonal bracing systems are the best model to minimize the base moment.

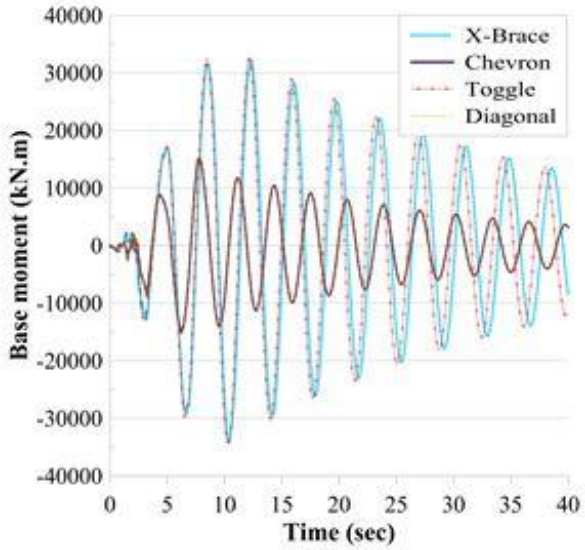

Figure 13. Time history of the base moment for different studied buildings

Fig. 14 plots the time history of base shear for different studied models. It can be seen that the chevron, toggle, and diagonal bracing systems are the best model to minimize the base shear.

Figs. (15-16) depict the time history of moment force for different studied models. It can be seen that the diagonal and chevron bracing systems are the best model to minimize the moment at the column located at the base and top floor of the building.

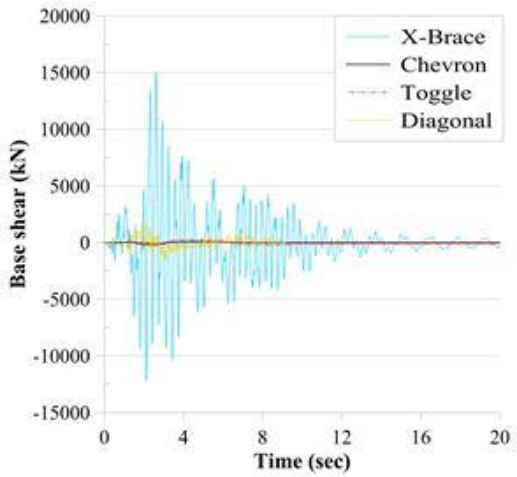

Figure 14. Time history of the base shear for different studied buildings

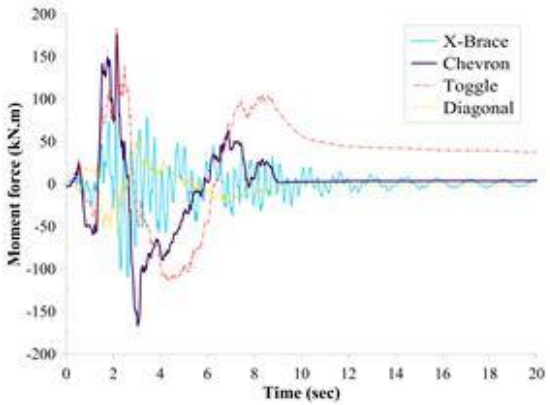

Figure 15. Time history of moment force for the column located at the base of the structure

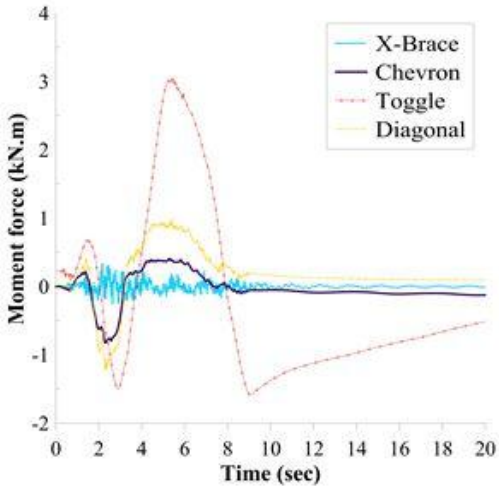

Figure 16. Time history of moment force for the column located at the top story

Figs. (17-18) show the time history of the shear force for different studied models. It can be seen that the toggle, chevron, and x-bracing systems are the best models to minimize the shear at the column located at the base and top floor of the building.

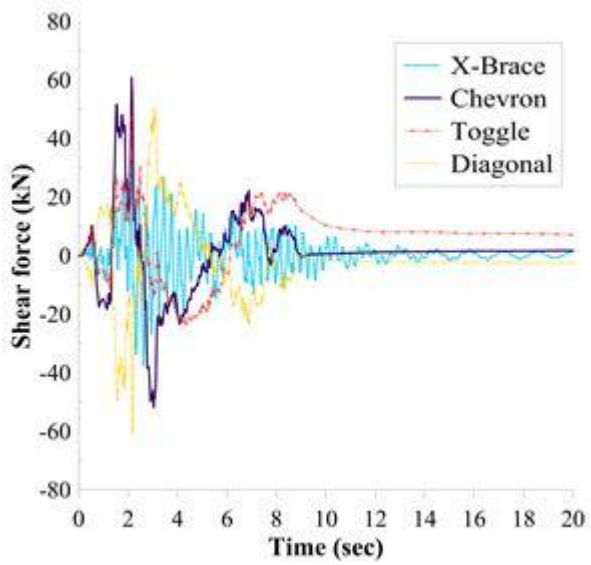

Figure 17. Time history of shear force for the column located at the base of the structure

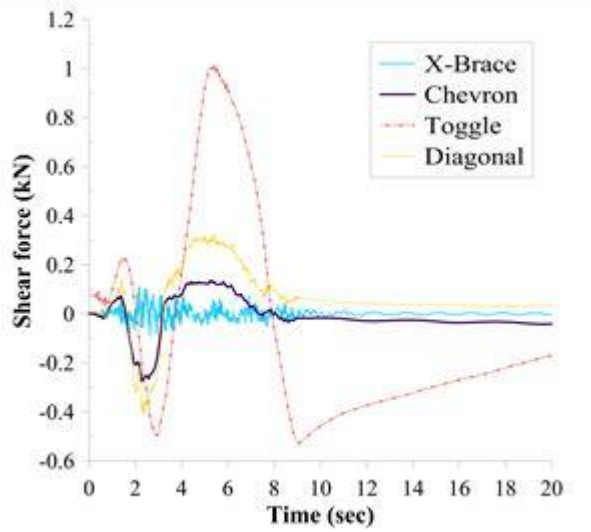

Figure 18. Time history of shear force for the column located at the top story

Fig. 19 shows the variation of shear force at a column for different elevations. It can be seen that the chevron and x-bracing systems are the best models to minimize the shear force.

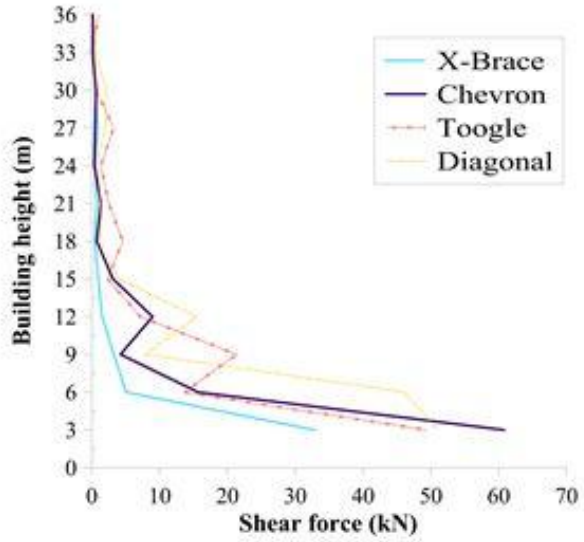

Figure 19. Variation of shear force at a column for different elevation

Fig. 20 shows the variation of moment force at a column for different elevations. It can be seen that the chevron and x-bracing systems are the best models to minimize the moment force.

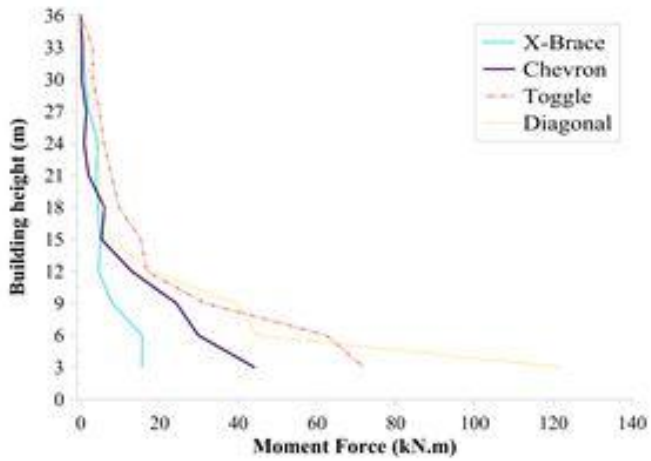

Figure 20. The variation of moment force at a column for different elevation

Fig. 21 shows the time history of axial force at a column located on the top floor. It can be seen that the chevron, toggle, and diagonal-bracing systems are the best models to minimize the axial force.

Fig. 22 presents the time history of axial force at a column located on the first story. It can be seen that the chevron, toggle, and diagonal-bracing systems are the best models to minimize the axial force.

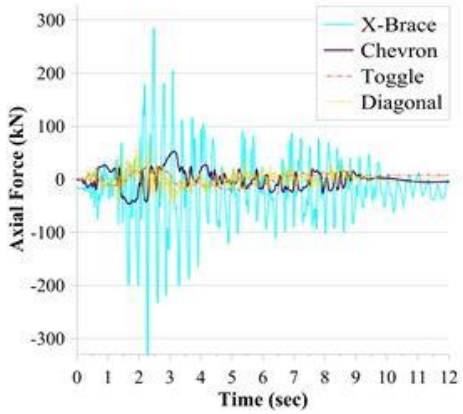

Figure 21. Time history of axial force at a column located on the top floor

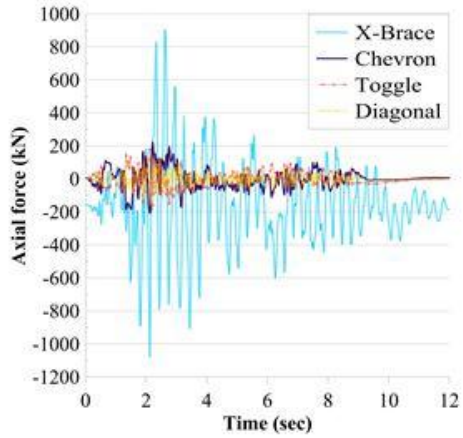

Figure 22. Time history of axial force at a column located on the first story

Figs. 23-26 show a comparison between the input, link damper, and modal damping energies for the diagonal, toggle, chevron, and X-bracing systems.

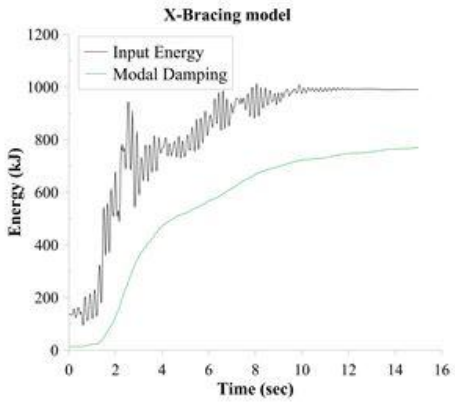

Figure 23. A comparison between the input and modal damping energies for the X-bracing system

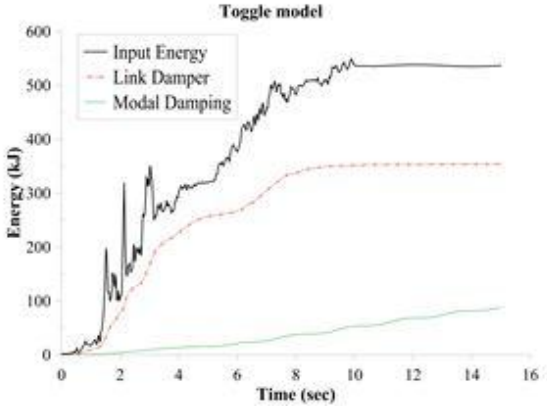

Figure 24. A comparison between the input, link damper and modal damping energies for the toggle-bracing system

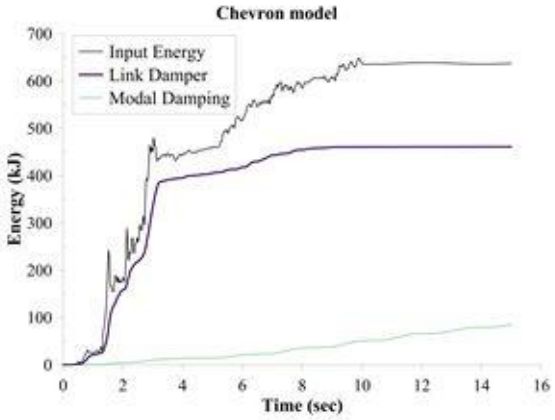

Figure 25. A comparison between the input, link damper and modal damping energies for the chevron-bracing system

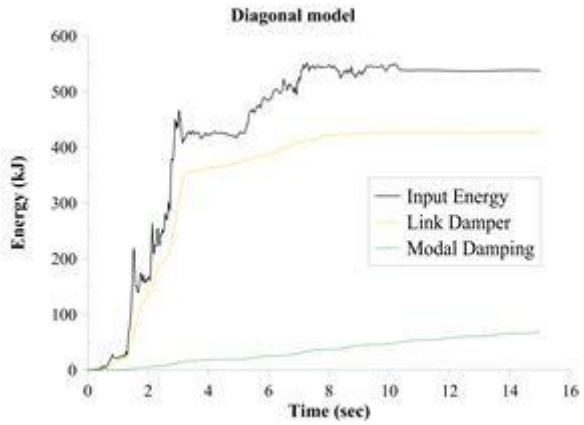

Figure 26. A comparison between the input, link damper and modal damping energies for the diagonal-bracing system

From Figs. (23-26), it can be seen that the diagonal bracing system has the best performance for increasing the modal damping energy dissipation because of absorbing more earthquake energy. Thus, lateral force is distributed uniformly between all elements and the base moment of diagonal decline.

Moreover, it is also apparent from Fig. 14 that the base shear capacity of diagonal is less than the X-bracing system. Besides, using FVD into the diagonal, chevron, and toggle bracing systems leads to drop down the values of base shear rapidly. This reduction saves on the construction of structural columns, foundations, and base plates because they have to endure a smaller amount of base shear.

The results show that the structures with the FVD have a better performance against the earthquake, so they absorb lower input energy rather than the X-bracing system (see Figs. 23 to 26). They also have fewer values of modal damping and more values of link damper rather than the X-bracing systems. Therefore, they can decrease the capacity of shear and moment for the members of the structure.

For the columns located on the first and top floors, the FVD system prevent the sharp variation for the moment force (see Figs. 15-16). However, the toggle bracing system is appropriate that reveal alternative behavior due to entering the structural elements to the plastic zone. A similar pattern can be seen for the columns located on the first and top floors related to the shear force (see Figs. 17-18). Besides, the nonstructural parts will have a slower vibration for the models equipped by FVD in comparison with the X-bracing system. From Figs. (18-26), it can be concluded that the chevron bracing system can absorb maximum values of input energy, shear, and moment forces.

Consequently, if Fig. 12 is considered, one of the most critical differences between the chevron and X-bracing system is related to roof displacement value. The values of roof displacement for the chevron bracing system is much lower than the X-bracing system.

Fig. 27 shows the inter-story drift hows inter-story drift for different models. The inter-story drift will reduce when the height of the structure increases for the controlled building with the FVD. It could be argued that FVD is one of the best dampers for a high-rise building.

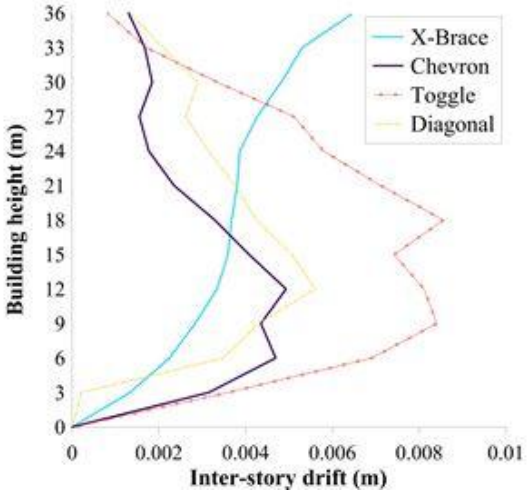

Figure 27. A comparison between the inter-story drift for different bracing systems

For the toggle bracing system, it has a downward trend at the end parts of the curve (see Fig. 27); therefore, after ending an earthquake, the structure will place in the elastic zone. Besides, considering the result of the X-bracing system shows that the use of this system in the tall building is a reason to create an upward trend for displacement. Figs. (23-26) show that a large part of input energy absorbs by FVD, which leads to creating a link damper energy. Also, by increasing the wavelength of responses in the axial forces (see Figs. 21-22) for toggle and chevron bracing systems, the structure can become more flexible than the diagonal bracing system. Overall, it can be concluded that the chevron and toggle bracing systems have a slowly reciprocating velocity than other studied models. Also, the chevron bracing system has a steady downward trend of damper forces when the hight of the building rises. It is due to the uniform distribution of lateral forces entire the structural height. Hence, the chevron bracing system equipped with the FVD system may be considered as the best option for a high-rise building.

The results of the present study demonstrate that the input energy for the X-bracing system is more than the other studied models (see Figs. 23-26). It proves the fact that the X-bracing system not only has a vast stiffness but also does not have damping constant. As a result, for toggle, chevron, and diagonal bracing systems, the formation of link damper could absorb 66%, 72%, and 79% of input energy instead of modal damping energy, respectively. Furthermore, the modal damping energy had a minimum contribution to the FVD models. Finally, it can be concluded that the FVD can dissipate massive energy that can be used to control the structural vibration during an earthquake.

6. CONCLUSIONS

The utilization of passive energy dissipation systems has been created a revolution in the structural engineering industry due to their advantages. Fluid Viscous Damper (FVD) is one of these control systems. In this paper, a comparison between the responses of a twelve-story steel building retrofitted by four layouts of bracings systems is studied. These bracing systems are equipped by FVD to find the optimum layout for these systems. Buildings are modeled nonlinearity and excited by an earthquake (Manjil earthquake) using SAP 2000 software. The results show that the toggle bracing system forces the structure to remain in the elastic zone after the earthquake. Besides, considering the result of the X-bracing system shows that the use of this system in the tall building is a reason to create an upward trend for displacement.

The results show that a large part of input energy absorbs by FVD, which leads to creating a link damper energy. Also, by increasing the wavelength of responses in the axial forces for toggle and chevron bracing systems, the structure can become more flexible than the diagonal bracing system. Overall, it can be concluded that the chevron and toggle bracing systems have a slowly reciprocating velocity than other studied models. Also, the chevron bracing system has a steady downward trend of damper forces when the hight of the building rises. It is due to the uniform distribution of lateral forces entire the structural height. Hence, the chevron bracing system equipped with the FVD system may be considered as the best option for a high-rise building. The results of the present study demonstrate that the input energy for the X-bracing system is more than the other studied

models. It proves the fact that the X-bracing system not only has a vast stiffness but also does not have damping constant. As a result, for toggle, chevron, and diagonal bracing systems, the formation of link damper could absorb 66%, 72%, and 79% of input energy instead of modal damping energy, respectively. Furthermore, the modal damping energy had a minimum contribution to the FVD models. Finally, it can be concluded that the FVD can dissipate massive energy that can be used to control the structural vibration during an earthquake.

REFERENCES

1. Kamgar R, Rahgozar P. Reducing static roof displacement and axial forces of columns in tall buildings based on obtaining the best locations for multi‐rigid belt truss outrigger systems, *Asian J Civil Eng* 2019; **20**: 759-768.
2. Fahimi Farzam M, Kaveh A. Optimum design of tuned mass dampers using colliding bodies optimization in frequency domain, *Iranian J Sci Technol, Transact Civil Eng* 2019. DOI: 10.1007/s40996-019-00296-6.
3. Kamgar R, Askari Dolatabad Y, Babadaei Samani M. Seismic optimization of steel shear wall using shape memory alloy, *Int J Optim Civil Eng* 2019; **9**(4): 671-87.
4. Kamgar R, Gholami F, Zarif Sanayei HR, Heidarzadeh H. Modified tuned liquid dampers for seismic protection of buildings considering soil–structure interaction effects, *Iranian J Sci Technol, Transact Civil Eng* 2020; **44**(1): 339-54.
5. Kamgar R, Khatibinia M, Khatibinia M. Optimization criteria for design of tuned mass dampers including soil–structure interaction effect, *Int J Optim Civil Eng* 2019; **9**(2): 213-22.
6. Kamgar R, Samea P, Khatibinia M. Optimizing parameters of tuned mass damper subjected to critical earthquake, *Struct Des Tall Special Build* 2018; **27**(7): e1460.
7. Kamgar R, Shojaee S, Rahgozar R. Rehabilitation of tall buildings by active control system subjected to critical seismic excitation, *Asian J Civil Eng* 2015; **16**(6): 819-33.
8. Kaveh A, Mohammadi S, Khadem Hosseini O, Keyhani A, Kalatjari VR. Optimum parameters of tuned mass dampers for seismic applications using charged system search, *Iranian J Sci Technol, Transact Civil Eng* 2015; **39**(C1): 21-40.
9. Kaveh A, Zakian P. Optimal seismic design of reinforced concrete shear wall-frame structures, *KSCE J Civil Eng* 2014; **18**(7): 2181-90.
10. Khatibinia M, Gholami H, Kamgar R. Optimal design of tuned mass dampers subjected to continuous stationary critical excitation, *Int J Dyn Control* 2018; **6**(3): 1094-1104.
11. Shayesteh Bilondi M R, Yazdani H, Khatibinia M. Seismic energy dissipation-based optimum design of tuned mass dampers, *Struct Multidisc Optim* 2018; **58**(6): 2517-31.
12. Tavakoli R, Kamgar R, Rahgozar R. The best location of belt truss system in tall buildings using multiple criteria subjected to blast loading, *Civil Eng J* 2018; **4**(6): 1338-53.
13. Tavakoli R, Kamgar R, Rahgozar R. Seismic performance of outrigger-braced system based on finite element and component-mode synthesis methods, *Iranian J Sci Technol,*

Transact Civil Eng 2019.
14. Tavakoli R, Kamgar R, Rahgozar R. Seismic performance of outrigger–belt truss system considering soil–structure interaction, *Int J Adv Struct Eng* 2019; **11**(1): 45-54.
15. Zamani AA, Tavakoli S, Etedali S. Control of piezoelectric friction dampers in smart base-isolated structures using self-tuning and adaptive fuzzy proportional–derivative controllers, *J Intell Mater Syst Struct* 2017; **28**(10): 1287-1302.
16. Zamani AA, Tavakoli S, Etedali S, Sadeghi J. Modeling of a magneto-rheological damper: An improved multi-state-dependent parameter estimation approach, *J Intell Mater Syst Struct* 2019; **30**(8): 1178-88.
17. Soong TT, Costantinou MC. *Passive and Active Structural Vibration Control in Civil Engineering,* Springer, Verlag Wien GmbH, New York, 2014.
18. Ras A, Boumechra N. Seismic energy dissipation study of linear fluid viscous dampers in steel structure design, *Alexandria Eng J* 2016; **55**(3): 2821-32.
19. Askari Dolatabad Y, Kamgar R, Gouhari Nezad I. Rheological and mechanical properties, acid resistance and water penetrability of lightweight self-compacting concrete containing nano-SiO2, nano-TiO2 and nano-Al2O3, *Iranian J Sci Technol, Transact Civil Eng* 2019; DOI: 10.1007/s40996-019-00328-1.
20. Kamgar R, Bagherinejad MH, Heidarzadeh H. A new formulation for prediction of the shear capacity of FRP in strengthened reinforced concrete beams, *Soft Comput* 2020; **24**: 6871-87.
21. Kamgar R, Hatefi SM, Majidi N. A fuzzy inference system in constructional engineering projects to evaluate the design codes for RC buildings, *Civil Eng J* 2018; **4**(9): 2155-72.
22. Kamgar R, Naderpour H, Ebrahimpour Komeleh H, Jakubczyk-Gałczyńska A, Jankowski R. A proposed soft computing model for ultimate strength estimation of FRP-confined concrete cylinders, *Appl Sci* 2020; **10**(5): 1769.
23. Kaveh A, Biabani Hamedani K, Hosseini SM, Bakhshpoori T. Optimal design of planar steel frame structures utilizing meta-heuristic optimization algorithms, *Struct* 2020; **25**: 335-46.
24. Kaveh A, Biabani Hamedani K, Zaerreza A. A set theoretical shuffled shepherd optimization algorithm for optimal design of cantilever retaining wall structures, *Eng Comput* 2020; DOI: 10.1007/s00366-020-00999-9.
25. Kaveh A, Izadifard R, Mottaghi L. Optimal design of planar RC frames considering CO2 emissions using ECBO, EVPS and PSO metaheuristic algorithms, *J Build Eng* 2020; **28**: 101014.
26. Kaveh A, Khodadadi N, Farahmand Azar B, Talatahari S. Optimal design of large-scale frames with an advanced charged system search algorithm using box-shaped sections, *Eng Comput* 2020; DOI: 10.1007/s00366-020-00955-7.
27. Rahmani F, Kamgar R, Rahgozar R. Optimum design of long-term deflection in segmented prestress bridges by considering the effects of creep and shrinkage, *Int J Optim Civil Eng* 2020; **10**(2): 315-31.
28. Lee D, Taylor DP. Viscous damper development and future trends, *Struct Des Tall Special Build* 2001; **10**(5): 311-20.

29. Ahmadi HR, Hamidi Jamnani H, Ghodrati Amiri GHR. The effect of analysis methods on the response of steel dual-system frame buildings for seismic retrofitting, *Int J Eng* 2009; **22**(4): 317-31.
30. Esmaeiltabar Nesheli P. Response modification factor of chevron braced frame with pall friction damper, *Int J Eng* 2013; **26**(2): 127-136.
31. Nateghi F. The effect of tuned mass damper on seismic response of building frames with uncertain structural characteristics, *Int J Eng* 2015; **28**(5): 662-670.
32. Nateghi F, Parsaeifard N. The effect of local damage on energy absorption of steel frame buildings during earthquake, *Int J Eng* 2013; **26**(2): 143-52.
33. Lian M, Su M, Guo Y. Seismic performance of eccentrically braced frames with high strength steel combination, *Steel Compos Struct* 2015; **18**(6): 1517-39.
34. Lian M, Su M, Guo Y. Experimental performance of Y-shaped eccentrically braced frames fabricated with high strength steel, *Steel Compos Struct* 2017; **24**(4): 441-53.
35. Lian M, Zhang H, Cheng Q, Su M. Finite element analysis for the seismic performance of steel frame-tube structures with replaceable shear links, *Steel Compos Struct* **2019**; **30**(4): 365-382.
36. Khatibinia M, Gholami H, Labbafi S. Multi–objective optimization of tuned mass dampers considering soil–structure interaction, *Int J Optim Civil Eng* 2016; **6**(4): 595-610.
37. Khatibinia M, Mahmoudi M, Elias H. Optimal sliding mode control for seismic control of buildings equipped with ATMD, *Int J Optim Civil Eng* 2020; **10**(1): 1-15.
38. Taylor DP. *History, Design, and Applications of Fluid Dampers in Structural Engineering*, in *Passive Structural Control Symposium*, Tokyo Institute of Technology, Tokyo, Japan, 2002.
39. Taylor DP, Constantinou MC. *Fluid Dampers for Applications of Seismic Energy Dissipation and Seismic Isolation*, Taylor Devices, Incorporated, 1998.
40. Monteiro MFS. Energy Dissipation System for Buildings, Instituto Superior Técnico, Technical University of Lisbon, 2011.
41. Martinez-Rodrigo M, Romero M. An optimum retrofit strategy for moment resisting frames with nonlinear viscous dampers for seismic applications, *Eng Struct* 2003; **25**(7): 913-25.
42. Kamgar R, Rahgozar R. A simple method for determining the response of linear dynamic systems, *Asian J Civil Eng* 2016; **17**(6): 801-785.
43. SAP2000. *Integrated Software for Structural Analysis and Design*, Available from: https://www.csiamerica.com, 2018.
44. ASCE-7-10, *Minimum Design Loads for Buildings and Other Structures*, American Society of Civil Engineers: Reston, Virginia, 2010.
45. PEER. *PEER Ground Motion Database*, Available from: https://ngawest2.berkeley.edu./2020.
46. ITT. *ITT Infrastructure Products*., Available from: www.itt-infrastructure.com, 2013.